



# Chemical Kinetic Modeling and Mass Spectrometric and Laser- Induced Fluorescence Measurements of $\text{NH}_3/\text{N}_2\text{O}$ Flames

by Demetris T. Venizelos and Rosario C. Sausa

## **NOTICES**

### **Disclaimers**

The findings in this report are not to be construed as an official Department of the Army position unless so designated by other authorized documents.

Citation of manufacturer's or trade names does not constitute an official endorsement or approval of the use thereof.

Destroy this report when it is no longer needed. Do not return it to the originator.

# Army Research Laboratory

Aberdeen Proving Ground, MD 21005-5066

---

ARL-TR-2782

July 2002

---

## Chemical Kinetic Modeling and Mass Spectrometric and Laser- Induced Fluorescence Measurements of $\text{NH}_3/\text{N}_2\text{O}$ Flames

Demetris T. Venizelos

National Research Council, ARL

Rosario C. Sausa

Weapons and Materials Research Directorate, ARL

---

Approved for public release; distribution is unlimited.

---

---

## Abstract

---

Experimental and chemical modeling studies of a 60-Torr,  $\text{NH}_3/\text{N}_2\text{O}/\text{Ar}$  flame are performed in order to provide further testing and refinements of a detailed chemical mechanism developed previously in our laboratory. This mechanism, which is denoted as VS, consists of 87 reactions and 20 species. Flame temperatures are measured with a coated thin-wire thermocouple and by rotational analyses of OH and NH laser-induced fluorescence (LIF) spectra. Species concentration profiles of  $\text{NH}_3$ ,  $\text{N}_2\text{O}$ ,  $\text{N}_2$ ,  $\text{H}_2\text{O}$ , NO,  $\text{O}_2$ , NH, O, and OH are recorded using molecular beam-mass spectrometry, LIF, or both. The experimental species concentrations are compared to those obtained with both equilibrium and PREMIX flame code calculations. The  $\text{NH}_3/\text{N}_2\text{O}$  mixture equilibrium calculations agree very well with both the PREMIX and measured postflame  $\text{N}_2$  and  $\text{H}_2\text{O}$  concentrations but underpredict the postflame NO concentration and overpredict the  $\text{O}_2$  concentration. The PREMIX calculations predict very well the shapes of the experimental  $\text{NH}_3$ ,  $\text{N}_2\text{O}$ ,  $\text{N}_2$ ,  $\text{H}_2\text{O}$ , NO, OH, and NH profiles throughout the flame but do not adequately predict the shape of the O-atom profile and overpredict the  $\text{O}_2$  concentration by ~60% at 16.25 mm, suggesting that the VS mechanism requires some refinement. A VS-modified mechanism, which provides better agreement with the experimental results, is proposed. In this mechanism, the rate constants of the following reactions are altered to the limit of their experimental or calculated uncertainties: (1)  $\text{N}_2\text{O} + \text{H} = \text{OH} + \text{N}_2$ , (2)  $\text{NH}_2 + \text{O} = \text{HNO} + \text{H}$ , (3)  $\text{NH}_2 + \text{OH} = \text{NH} + \text{H}_2\text{O}$ , (4)  $\text{NH}_2 + \text{H} = \text{H}_2 + \text{NH}$ , (5)  $\text{NH}_3 + \text{OH} = \text{NH}_2 + \text{H}_2\text{O}$ , and (6)  $\text{NO} + \text{H} + \text{M} = \text{HNO} + \text{M}$ .

---

## Acknowledgments

---

This work was supported by the U.S. Army Research Laboratory (ARL) Mission Program on Combustion and the National Research Council ARL Postdoctoral Fellowship Program.

INTENTIONALLY LEFT BLANK.

---

## Contents

---

|                                  |            |
|----------------------------------|------------|
| <b>Acknowledgments</b>           | <b>iii</b> |
| <b>List of Figures</b>           | <b>vii</b> |
| <b>List of Tables</b>            | <b>ix</b>  |
| <b>1. Introduction</b>           | <b>1</b>   |
| <b>2. Experimental/Modeling</b>  | <b>2</b>   |
| <b>3. Results/Discussion</b>     | <b>3</b>   |
| <b>4. Conclusion</b>             | <b>12</b>  |
| <b>5. References</b>             | <b>13</b>  |
| <b>Distribution List</b>         | <b>15</b>  |
| <b>Report Documentation Page</b> | <b>17</b>  |

INTENTIONALLY LEFT BLANK.

---

## List of Figures

---

|  |    |
|--|----|
| Figure 1. Experimental (....) and fitted (-) NH spectra of a 60-Torr, NH <sub>3</sub> /N <sub>2</sub> O/ Ar flame in the region of 302.2–302.7 nm. The experimental data is recorded at 5.5 mm above the burner surface. ....  | 4  |
| Figure 2. Temperature profiles of a 60-Torr, NH <sub>3</sub> /N <sub>2</sub> O/ Ar flame obtained by OH LIF (o), NH LIF (◄) and a thin-wire thermocouple (O). The thermocouple temperatures are corrected for radiation losses using the LIF temperatures. ....  | 4  |
| Figure 3. Pathway diagram of a 60-Torr, NH <sub>3</sub> /N <sub>2</sub> O/ Ar flame generated by integrating the net rate fluxes of the individual reactions from the burner surface to 30 mm ( $100 = 2.716 \text{ H}10^{-5} \text{ mol/cm}^2\text{-s}$ ). For NNH destruction, $\vartheta + \text{M}$ indicates the total predissociation and collision-assisted decomposition. ....                               | 8  |
| Figure 4. Normalized experimental and modeled OH and NH profiles of the 60-Torr, NH <sub>3</sub> /N <sub>2</sub> O flame. The OH mole fractions at 15 mm are $6.0 \text{ H}10^{-3}$ and $3.9 \text{ H}10^{-3}$ for VS and VS-modified calculations, respectively, and those of NH at the peak value are $5.7 \text{ H}10^{-4}$ and $3.7 \text{ H}10^{-4}$ for the VS and VS-modified calculations, respectively..... | 9  |
| Figure 5. Experimental and modeled NO profiles of the 60-Torr, NH <sub>3</sub> /N <sub>2</sub> O/ Ar flame. The experimental profiles are obtained by MB-MS (O) and LIF (B).....   | 10 |
| Figure 6. Experimental and modeled O <sub>2</sub> profiles of the 60-Torr, NH <sub>3</sub> /N <sub>2</sub> O/ Ar flame.....  | 11 |

INTENTIONALLY LEFT BLANK.

---

## List of Tables

---

|  |   |
|--|---|
| Table 1. Sensitivity coefficients of O <sub>2</sub> for the NH <sub>3</sub> /N <sub>2</sub> O/Ar and H <sub>2</sub> N <sub>2</sub> O/Ar flames using the VS mechanism at 15.0 mm above the burner surface. ....      | 6 |
| Table 2. Rate expressions of reactions altered for the VS-modified mechanism. The rate coefficients are in the form $K = AT^b e^{-E/RT}$ , where $A$ and $E$ have units of cm/mol/s/K and cal/mol, respectively..... | 7 |

INTENTIONALLY LEFT BLANK.

---

## 1. Introduction

---

The H<sub>2</sub>/N<sub>2</sub>O chemical system has been the subject of numerous studies because it is fairly simple and because it has important implications in understanding NO<sub>x</sub> pollutant formation and nitramine propellant combustion and decomposition [1–4]. The elementary reactions of the system form subsets of larger mechanisms needed to understand the nitrogen chemistry of more complex combustion systems. Recently, we reported on a combined experimental and modeling flame structure study of both neat and NH<sub>3</sub>-doped (4%) H<sub>2</sub>/N<sub>2</sub>O/Ar flames [1]. The species mole fractions were measured by molecular beam-mass spectrometry (MB-MS) and laser-induced fluorescence (LIF) and then compared to those calculated by PREMIX using both the Sausa, Singh, Lemire, and Anderson (SSLA) [2] and Gas Research Institute (GRI) 2.11 mechanisms [5]. The SSLA mechanism was developed in-house from a critical literature review, whereas the GRI 2.11 mechanism was developed by a consortium of scientists for GRI for natural gas ignition and flame. Overall, the calculations using both mechanisms adequately predicted the profiles of the major species for both the neat and NH<sub>3</sub>-doped flame. However, both mechanisms failed to predict the postflame O<sub>2</sub> concentration in the neat flame, the drop in the O<sub>2</sub> concentration with the addition of NH<sub>3</sub>, and the NH<sub>3</sub> decay in the doped flame. A modified SSLA mechanism, which provided better agreement with our experimental data, was proposed. This mechanism is denoted as “VS” in this report, and a list of the chemical reactions and their corresponding rate expressions is presented in Venizelos and Sausa [1] and Sausa et al. [2].

In this report, we provide a combined experimental and chemical modeling study of a stoichiometric NH<sub>3</sub>/N<sub>2</sub>O/Ar flame in order to provide further testing and refinements of the VS chemical mechanism. Species concentration profiles are recorded by MB-MS, LIF, or both, and flame temperatures are measured by thin-wire thermometry and by OH and NH LIF. The experimental mole fractions are compared to those predicted by both equilibrium calculations and PREMIX calculations using the VS chemical mechanism. The PREMIX results adequately predict all of the measured species profiles except for the O-atom and O<sub>2</sub> profiles. A refined mechanism, denoted VS-modified, which better predicts our experimental results, is proposed. In this mechanism, six reactions are identified that may need new rate-constant measurements under conditions of temperature and pressure that are similar to our flame conditions.

---

## 2. Experimental/Modeling

---

The low-pressure burner assembly and the procedures for the LIF and MB-MS measurements are described elsewhere [1, 2]. Briefly, a 60-Torr,  $\text{NH}_3/\text{N}_2\text{O}/\text{Ar}$  flame is supported on a water-cooled, stainless steel, McKenna flat burner, which is mounted in a cylindrical vacuum chamber. Translation of the burner provides full optical access to the flame. The gas flow rates for  $\text{NH}_3$ ,  $\text{N}_2\text{O}$ , and Ar are 1.03, 1.59, and 0.54 slm, respectively. The experimental apparatus is configured so that the LIF and thermocouple measurements are recorded exactly where the MB-MS probe was sampling, allowing for direct comparison.

Flame temperatures are measured with a coated, thin-wire Pt-Rh (6%)/Pt-Rh (30%) thermocouple and by NH and OH LIF. Measuring the flame temperatures as a function of height above the burner surface yields a thermocouple temperature profile, which is then corrected for thermocouple radiation losses by OH and NH LIF. The LIF temperatures are determined by a Boltzmann rotational population distribution analysis of the recorded spectra using a computer program with interactive graphics [1]. All of the temperature data are fitted with a sigmoid-type function and used as input in the PREMIX calculations. The overall uncertainty in the NH and OH LIF temperature measurements is  $\pm 2$  and  $\pm 5\%$  (2SD), respectively.

The MB-MS species profiles are quantified using a calibration procedure previously described [1, 2]. As it is difficult to reliably introduce a calibrated amount of  $\text{H}_2\text{O}$  vapor in the burner system, the  $\text{H}_2\text{O}$  mole fraction is determined by balancing the N/O ratio in the premixed inlet gases to the ratio of N/O in the burnt gases. The resulting expression for the mole fraction ratio of  $\text{H}_2\text{O}$  to Ar in the postflame region is

$$X_{\text{H}_2\text{O}}/X_{\text{Ar}} = 6/8 (X_{\text{N}_2}/X_{\text{Ar}}) + 5/8 (X_{\text{NO}}/X_{\text{Ar}}) + 2 (X_{\text{O}_2}/X_{\text{Ar}}), \quad (1)$$

where the values of  $X_{\text{N}_2}/X_{\text{Ar}}$ ,  $X_{\text{NO}}/X_{\text{Ar}}$ , and  $X_{\text{O}_2}/X_{\text{Ar}}$  are measured experimentally. It is assumed that the concentration of the other species in the burnt gases is much less than the concentrations of the species shown in equation 1; thus, they do not contribute to the  $X_{\text{H}_2\text{O}}/X_{\text{Ar}}$  ratio. NASA-Lewis equilibrium calculations of  $\text{NH}_3$  and  $\text{N}_2\text{O}$  mixtures [6] and experimental MB-MS species observations or lack thereof support this assumption. The uncertainty in the MB-MS measurements is 10%.

We model the flames with the Sandia National Laboratories (SNL) flame code PREMIX (ver. 2.55) [7] employing the CHEMKIN-II mechanism interpreter (ver. 3.6) and chemical kinetics libraries (ver. 4.9) [8]. The SNL thermodynamic [9] and transport property databases [10], our measured temperature and flow rates,

and our VS chemical mechanism are used as input. Both the thermal diffusion and multicomponent transport package options are included in the calculations. The VS chemical mechanism consists of 87 reactions and 20 species [1, 2]. The bulk of the reactions are obtained from the benchmark review of nitrogen chemistry in combustion by Miller and Bowman [11]. The mechanism also includes the results of Hanson and coworkers for many important reactions involving NH<sub>x</sub> species that were poorly quantified [12, 13] and some reactions from a nitrogen chemistry review by Bozzelli and Dean, which relate to their recommended NO formation mechanism [14]. An interactive post-processing code written in-house is used for the rate and sensitivity analyses [15].

---

### 3. Results/Discussion

---

The flame temperatures are measured by OH and NH LIF. Figure 1 shows the experimental and fitted NH LIF spectra in the region of 302.2–302.7 nm. The experimental spectra are recorded in a linear laser energy regime and normalized with respect to the laser energy. Quenching effects and laser intensity fluctuation errors are minimized by using a short 9-ns gated integrator and 10-shot averaging. A multiparameter computer program based on a Boltzmann rotational distribution analyses fits the observed data [1]. The program utilizes one-photon line strengths and rotational energy levels of NH obtained from Brazier et al. [16], and OH from Dieke and Crosswhite [17] and Dimpfl and Kinsey [18]. Parameters include laser line shape, temperature, and absolute and relative frequency values for the data. Doppler and collisional broadening is also accounted by the fitting routine. The standard deviation of each parameter, as statistically determined from the fit, is obtained from the computer variance-covariance matrix once convergence is achieved. The best fit to the observed data using a Gaussian function laser line shape yields a temperature of 2012 K  $\pm$  50 K (2SD) at 5.5 mm above the burner surface.

Presented in Figure 2 are the flame temperatures measured by OH and NH LIF and a coated thin-wire thermocouple. The thermocouple temperatures are corrected for radiation losses using the OH LIF temperatures in the postflame region and NH LIF temperatures near the burner surface and in the preheat flame region, similar to a procedure used for a H<sub>2</sub>/N<sub>2</sub>O/Ar flame [1]. The corrected thermocouple temperature profiles are then fitted with a sigmoid-type function and used in the PREMIX calculations. As shown in Figure 2, the temperature profile peaks at  $\sim$ 2200 K near 7 mm above the burner surface.

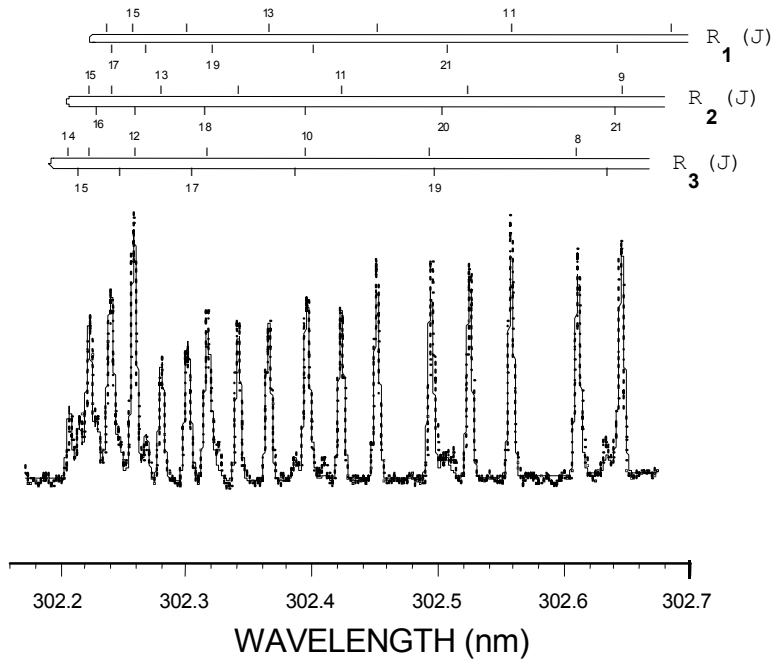


Figure 1. Experimental (...) and fitted (-) NH spectra of a 60-Torr,  $\text{NH}_3/\text{N}_2\text{O}/\text{Ar}$  flame in the region of 302.2–302.7 nm. The experimental data is recorded at 5.5 mm above the burner surface.

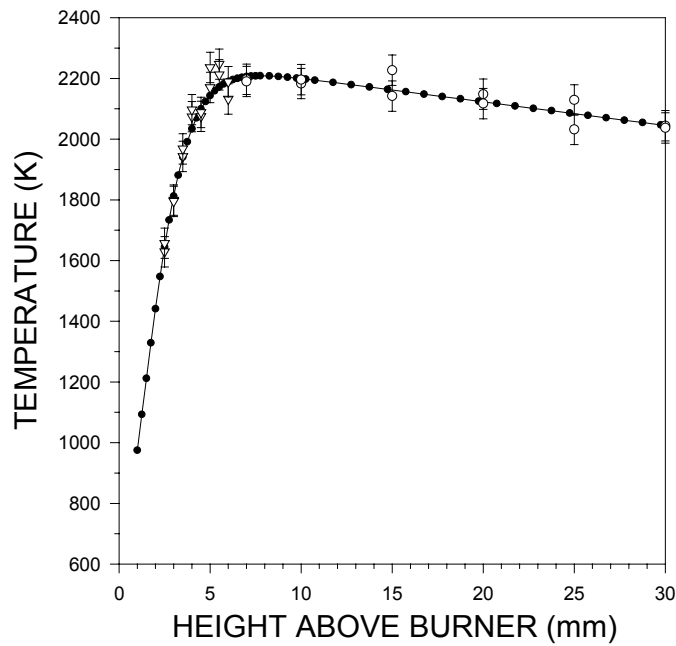


Figure 2. Temperature profiles of a 60-Torr,  $\text{NH}_3/\text{N}_2\text{O}/\text{Ar}$  flame obtained by OH LIF (o), NH LIF ( $\triangle$ ), and a thin-wire thermocouple (O). The thermocouple temperatures are corrected for radiation losses using the LIF temperatures.

The PREMIX calculations using the VS mechanism predict very well the  $\text{NH}_3$ ,  $\text{N}_2\text{O}$ ,  $\text{N}_2$ ,  $\text{H}_2\text{O}$ , and  $\text{NO}$  mole fractions and the shapes of the  $\text{OH}$  and  $\text{NH}$  species throughout the flame. However, they overpredict the  $\text{O}_2$  mole fraction by about a factor of 2 in the burned region of the flame and do not adequately predict the O-atom profile (these results will be discussed in more detail later). These discrepancies are not due to temperature effects because a 5% decrease in the inputted temperature profile, the maximum uncertainty in our temperature measurements, decreases the  $\text{O}_2$  postflame mole fraction by <3% and does not significantly change the shape of the O-atom profile. Similar calculations performed on a neat and  $\text{NH}_3$ -doped  $\text{H}_2/\text{N}_2\text{O}/\text{Ar}$  flame predict the  $\text{O}_2$  mole fraction in the burned region of both flames within a few percent [1]. They also predict that the  $\text{O}_2$  postflame mole fraction in the neat flame decreases by 84% when the flame is doped with 4%  $\text{NH}_3$ , in excellent agreement with the observed 90% decrease [1]. This suggests that the discrepancy between the observed and calculated O-atom and  $\text{O}_2$  profiles in the  $\text{NH}_3/\text{N}_2\text{O}/\text{Ar}$  flame is due to the model rather than the experiment and that the VS mechanism requires some refinement.

Sensitivity analyses of the PREMIX results reveal which reactions in the VS mechanism need to be altered to better predict the experimental species profiles. The normalized sensitivity coefficients for  $\text{O}_2$  at 15.0 mm above the burner surface for the  $\text{NH}_3/\text{N}_2\text{O}/\text{Ar}$  flame are presented in Table 1. All of the sensitivity coefficients are normalized logarithmically using the maximum  $\text{O}_2$  mole fraction and then scaled to the  $\text{NH} + \text{OH} = \text{HNO} + \text{H}$  reaction (R1). Table 1 reveals that  $\text{O}_2$  has a very strong negative sensitivity to reactions R1, R3, R4, and R6 and a positive sensitivity to reactions R2 and R5. Negative sensitivity values indicate that an increase in the reaction rate results in a decrease in the  $\text{O}_2$  mole fraction, whereas positive values indicate that an increase in the reaction rate results in an increase in the  $\text{O}_2$  mole fraction. Similar analyses for the  $\text{H}_2/\text{N}_2\text{O}/\text{Ar}$  flame reveal that  $\text{O}_2$  is also very sensitive to all of these reactions except reaction R3 (see Table 1). Also, reaction R4 shows a positive sensitivity coefficient value, different from that in the  $\text{NH}_3/\text{N}_2\text{O}/\text{Ar}$  flame. These sensitivity analyses suggest that an increase in the rate expression of both R3 and R4 will decrease the postflame  $\text{O}_2$  mole fraction in the  $\text{NH}_3/\text{N}_2\text{O}/\text{Ar}$  flame and, overall, slightly increase the  $\text{O}_2$  mole fraction in the  $\text{H}_2/\text{N}_2\text{O}/\text{Ar}$  flame. This is consistent with our present experimental results and those previously published [1]. An increase in the rate of R4 also decreases the  $\text{NO}$  postflame concentration, consistent with our present experimental results (sensitivity results for  $\text{NO}$  are not shown). However, a large increase in this reaction is not warranted because it would reduce the  $\text{NO}$  mole fraction more than what we observe experimentally. Thus, a 10% increase is proposed. This is within the experimental limits of the rate expression reported by Marshall et al. [19]. A very large increase in the rate of R3 increases the postflame  $\text{NO}$  mole fraction, contrary to what is observed experimentally. Thus, its rate expression is only increased by 50%, in line with our experimental results, the experimental

Table 1. Sensitivity coefficients of O<sub>2</sub> for the NH<sub>3</sub>/N<sub>2</sub>O/Ar and H<sub>2</sub>N<sub>2</sub>O/Ar flames using the VS mechanism at 15.0 mm above the burner surface.

| Reaction |   | NH <sub>3</sub> /N <sub>2</sub> O/Ar |       | H <sub>2</sub> /N <sub>2</sub> O/Ar |       |
|----------|---|--------------------------------------|-------|-------------------------------------|-------|
|          |   | Sign                                 | %     | Sign                                | %     |
| R1       | NH + OH = HNO + H   | (-)                                  | 100.0 | (-)                                 | 100.0 |
| R2       | N <sub>2</sub> O + M = N <sub>2</sub> + O + M             | (+)                                  | 77.7  | (+)                                 | 266.4 |
| R3       | NH <sub>2</sub> + O = HNO + H                             | (-)                                  | 76.0  | (-)                                 | 4.0   |
| R4       | N <sub>2</sub> O + H = OH + N <sub>2</sub>                | (-)                                  | 66.0  | (+)                                 | 26.7  |
| R5       | NO + N = N <sub>2</sub> + O                               | (+)                                  | 58.6  | (+)                                 | 85.2  |
| R6       | NO + H = N + OH   | (-)                                  | 49.3  | (-)                                 | 78.3  |
| R7       | NH <sub>2</sub> + OH = NH + H <sub>2</sub> O              | (+)                                  | 37.9  |                                     | <3.0  |
| R8       | NNH + O = NO + NH   | (+)                                  | 36.8  | (+)                                 | 42.4  |
| R9       | NH + NO = N <sub>2</sub> + OH                             | (+)                                  | 34.8  | (+)                                 | 33.6  |
| R10      | NH + O = NO + H   | (-)                                  | 30.4  | (-)                                 | 39.8  |
| R11      | NH <sub>2</sub> + NO = NNH + OH                           | (+)                                  | 27.8  |                                     | < 3.0 |
| R12      | NH <sub>3</sub> + OH = NH <sub>2</sub> + H <sub>2</sub> O | (+)                                  | 26.1  |                                     | < 3.0 |
| R13      | NH <sub>2</sub> + NO = N <sub>2</sub> + H <sub>2</sub> O  | (+)                                  | 20.1  |                                     | < 3.0 |
| R14      | NH <sub>2</sub> + H = NH + H <sub>2</sub>                 | (+)                                  | 19.2  |                                     | < 3.0 |
| R15      | NH + NO = N <sub>2</sub> O + H                            | (-)                                  | 16.2  | (-)                                 | 73.5  |
| R16      | H + O <sub>2</sub> = OH + O                               | (+)                                  | 14.1  | (+)                                 | 18.7  |
| R17      | NO + H + M = HNO + M                                      | (+)                                  | 12.4  | (+)                                 | 3.4   |
| R18      | N <sub>2</sub> O + O = NO + NO                            | (-)                                  | 10.8  | (-)                                 | 24.2  |
| R19      | OH + OH = H <sub>2</sub> O + O                            | (+)                                  | 6.9   |                                     | < 3.0 |
| R20      | NH <sub>3</sub> + H = NH <sub>2</sub> + H <sub>2</sub>    | (+)                                  | 6.1   |                                     | < 3.0 |
| R21      | HNO + OH = NO + H <sub>2</sub> O                          | (-)                                  | 6.1   |                                     | < 3.0 |
| R22      | H <sub>2</sub> + OH = H <sub>2</sub> O + H                | (-)                                  | 6.0   | (-)                                 | 21.2  |
| R23      | HNO + H = NO + H <sub>2</sub>                             | (-)                                  | 5.3   | (-)                                 | 6.0   |

Notes: The sensitivity coefficients are normalized logarithmically using the maximum O<sub>2</sub> mole fraction and scaled to the NH + OH = HNO + H reaction.

NH<sub>3</sub>/N<sub>2</sub>O/Ar flame: 100 units = 0.20239.

H<sub>2</sub>/N<sub>2</sub>O/Ar flame: 100 units = 0.5508.

uncertainty in the reported rate expression, and the uncertainty in the rate expression of R4. Reactions R4 and R3, along with their original and altered rate expressions, are presented in Table 2 as part of a refined VS-mechanism, denoted as VS-modified.

O<sub>2</sub> has an appreciable positive sensitivity to several reactions in an NH<sub>3</sub>/N<sub>2</sub>O/Ar flame which do not influence the postflame O<sub>2</sub> concentration much in an H<sub>2</sub>/N<sub>2</sub>O/Ar flame. These reactions, which are listed in Table 1, are R7, R11, R12, R13, R14, and R17. Altering these reactions does not considerably influence the postflame NO mole fraction for both H<sub>2</sub>/N<sub>2</sub>O/Ar and NH<sub>3</sub>/N<sub>2</sub>O/Ar flames; thus, an increase in their rate expression would better predict our experimental results. Only reactions R7, R12, R14, and R17 are recommended for further study because reactions R11 and R3 are well established over a wide range of

Table 2. Rate expressions of reactions altered for the VS-modified mechanism. The rate coefficients are in the form  $K = AT^B e^{(-E/RT)}$ , where  $A$  and  $E$  have units of  $\text{cm}^3/\text{mol}/\text{s}/\text{K}$  and  $\text{cal}/\text{mol}$ , respectively.

| Reaction |  | VS      |        |         | VS-Modified |            |         |           |
|----------|--|---------|--------|---------|-------------|------------|---------|-----------|
|          |  | A       | B      | E       | A           | B          | E       | Reference |
| R4       | $\text{N}_2\text{O} + \text{H} = \text{OH} + \text{N}_2$     | 2.53E10 | 0.0    | 4550.0  | 2.78E10     | 0.0        | 4550.0  | [19]      |
|          |  | 2.23E14 | 0.0    | 16750.0 | 2.45E14     | 0.0        | 16750.0 | [19]      |
| R3       | $\text{NH}_2 + \text{O} = \text{HNO} + \text{H}$             | 4.60E13 | 0.0    | 0.0     | 6.90E13     | 0.0        | 0.0     | [20]      |
| R7       | $\text{NH}_2 + \text{OH} = \text{NH} + \text{H}_2\text{O}$   | 4.00E06 | 2.0    | 1000.0  | 2.00E06     | 2.0        | 1000.0  | [11]      |
| R12      | $\text{NH}_3 + \text{OH} = \text{NH}_2 + \text{H}_2\text{O}$ | 2.04E06 | 2.04   | 566.0   | 1.04E06     | 2.04       | 566.0   | [11]      |
| R14      | $\text{NH}_2 + \text{H} = \text{NH} + \text{H}_2$            | 4.00E13 | 0.0    | 3650.0  | 1.33E13     | 0.0        | 3650.0  | [13]      |
| R17      | $\text{NO} + \text{H} + \text{M} = \text{HNO} + \text{M}$    | 9.00E19 | ! 1.30 | 735.0   | 3.00E19     | ! 1.3<br>0 | 735.0   | [21]      |

temperatures and their branching ratio is well characterized [22, 23]. Reactions R7, R12, R14, and R17, together with their original and altered rate expressions, are also presented in Table 2 as part of the VS-modified mechanism.

PREMIX calculations using the VS-modified mechanism are also performed for the  $\text{NH}_3/\text{N}_2\text{O}/\text{Ar}$  flame in order to test the proposed mechanism. The measured temperature profile is used as input into the flame code; however, it is decreased by 5%, the experimental uncertainty. The resulting profiles are then compared to those obtained experimentally and to those obtained from PREMIX using the VS mechanism and measured temperature profile as input. The VS-modified calculations predict very well the  $\text{NH}_3$ ,  $\text{N}_2\text{O}$ ,  $\text{H}_2\text{O}$ , and  $\text{N}_2$  species mole fraction throughout the flame, as do the VS calculations. At 16.25 mm above the burner surface, the calculations predict within 1% the observed  $\text{H}_2\text{O}/\text{Ar}$  and  $\text{N}_2/\text{Ar}$  values of 3.83 and 2.76, respectively. For comparison, NASA-Lewis equilibrium calculations also predict the major species mole fraction within 1% in the burned gas region of the flame.

Figure 3 is a pathway diagram of the VS-modified results showing the nitrogen chemistry occurring in the  $\text{NH}_3/\text{N}_2\text{O}/\text{Ar}$  flame. The numbers in parentheses are the relative integrated net reaction rates from 0 to 30.0 mm for the disappearance of the indicated reactant by the various reactions. These integrated rates are normalized to 100 ( $2.55 \times 10^{-5} \text{ mol}/\text{cm}^2\text{-s}$ ) for the  $\text{NH}_3 + \text{OH} = \text{NH}_2 + \text{H}_2\text{O}$  reaction. The  $\text{N}_2\text{O}$  reactant is consumed primarily by reactions with H and M to form  $\text{N}_2$ , whereas its companion reactant,  $\text{NH}_3$ , is consumed by reactions involving the OH, H, and O species to form  $\text{NH}_2$ . To some extent,  $\text{NH}_3$  is regenerated mainly from  $\text{NH}_2$  species reacting with themselves. Although the reactions involving  $\text{N}_2\text{O}$  with H and M are the major routes for  $\text{N}_2$  formation, ~32% of  $\text{N}_2$  is formed from the  $\text{NNH}$ ,  $\text{NH}_2$ ,  $\text{NH}$ ,  $\text{NO}$ , and  $\text{N}$  species.

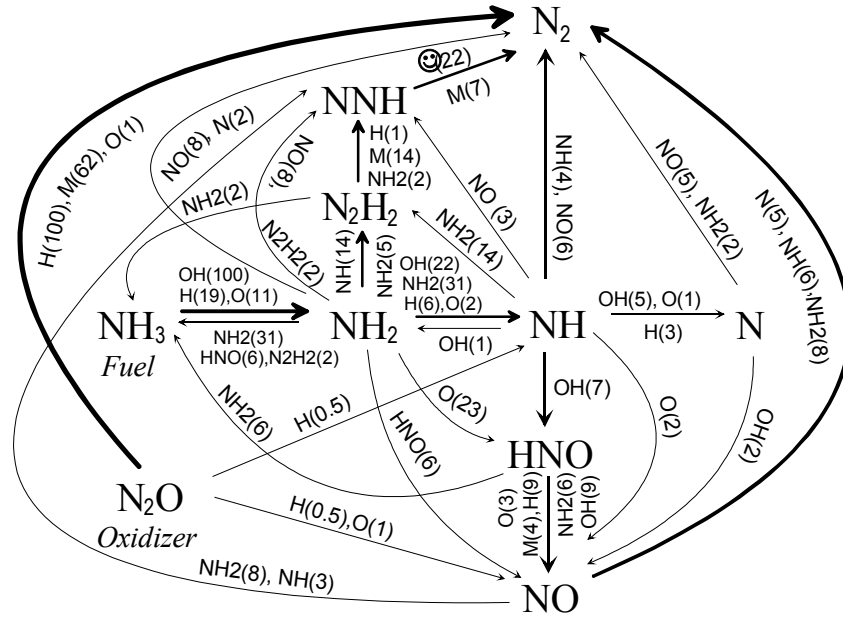


Figure 3. Pathway diagram of a 60-Torr, NH<sub>3</sub>/N<sub>2</sub>O/Ar flame generated by integrating the net rate fluxes of the individual reactions from the burner surface to 30 mm (100 = 2.716 H 10<sup>-5</sup> mol/cm<sup>2</sup>-s). For NNH destruction, 9 + M indicates the total predissociation and collision-assisted decomposition.

Figure 4 shows the experimental and modeled NH and OH profiles. The experimental LIF concentrations are converted to mole fractions using the measured flame temperatures and then normalized to the calculated mole fractions for comparison purposes. The OH profile is predicted extremely well in the region near the burner surface and the postflame region by the PREMIX calculations using both the VS and VS-modified mechanisms. The NH LIF profile reaches its peak value at 3.75 mm above the burner surface, compared to the VS and VS-modified calculation profiles which peak at 4 and 4.5 mm, respectively. A narrower width in the NH profile is also observed experimentally (full width at half maximum [FWHM] = 2.5 mm). In contrast, the VS and VS-modified calculations predict a width (FWHM) of 3 and 4 mm, respectively.

Rate analysis of the VS-modified results reveals that NH is formed predominantly from NH<sub>2</sub> reacting with OH, H, and NH<sub>2</sub>, and that it is consumed either directly to N<sub>2</sub>, N<sub>2</sub>H<sub>2</sub>, NNH, and HNO or indirectly to N by means of the NH intermediate (see Figure 3). A similar analysis for OH reveals that over 88% of this species is formed from the N<sub>2</sub>O + H = OH + N<sub>2</sub> and OH + OH = H<sub>2</sub>O + O reactions, and that more than 59% is consumed from the NH<sub>3</sub> + OH = NH<sub>2</sub> + H<sub>2</sub>O reaction. The reactions H<sub>2</sub> + OH = H<sub>2</sub>O + H, NH<sub>2</sub> + OH = H<sub>2</sub>O + NH, HNO + OH = NO + H<sub>2</sub>O, and NH + OH = HNO + H account for ~40% of its consumption.

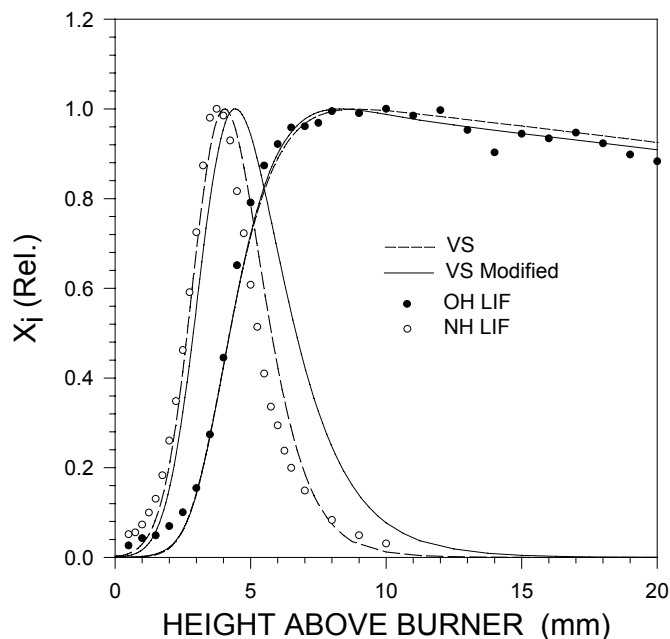


Figure 4. Normalized experimental and modeled OH and NH profiles of the 60-Torr,  $\text{NH}_3/\text{N}_2\text{O}$  flame. The OH mole fractions at 15 mm are  $6.0 \times 10^{-3}$  and  $3.9 \times 10^{-3}$  for VS and VS-modified calculations, respectively, and those of NH at the peak value are  $5.7 \times 10^{-4}$  and  $3.7 \times 10^{-4}$  for the VS and VS-modified calculations, respectively.

Figure 5 shows the PREMIX calculated and experimental MB-MS and LIF profiles of NO. The NO LIF species concentration profile is converted to a NO/Ar mole fraction ratio using the measured temperatures and the calculated Ar mole fraction. Its peak concentration is normalized to the calibrated MB-MS peak value for comparison purposes. Figure 4 shows that the LIF and MB-MS profiles have the same shape. Also, the VS and VS-modified calculations predict very well the measured NO/Ar profiles throughout the flame, overestimating the value of the NO/Ar ratio at 16.25 mm only by about 7 and 10%, respectively. These values are within the uncertainty of the MB-MS measurements. NASA-Lewis equilibrium calculations underpredict the NO/Ar by a factor of 10, indicating that NO is not in equilibrium and is preventing full energy release of the system. The pathway diagram presented in Figure 3 shows that NO is formed predominantly from the intermediates HNO,  $\text{NH}_2$ , N, and NH. The  $\text{N}_2\text{O}$  reactant is not an important source of NO in this flame as it is in the neat and  $\text{NH}_3$ -doped  $\text{H}_2/\text{NO}/\text{Ar}$  flames [1, 2]. NO is converted to  $\text{N}_2$  directly by the N, NH, and  $\text{NH}_2$  intermediates or indirectly by the NNH intermediate.

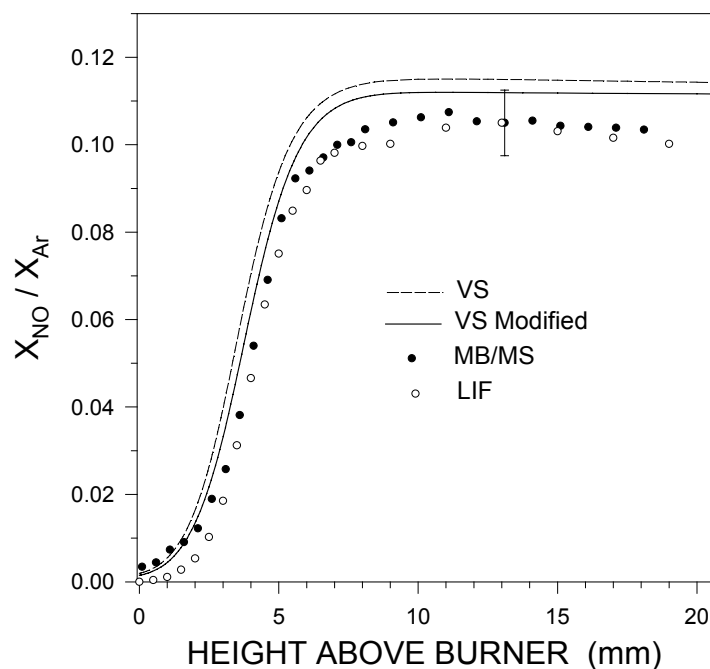


Figure 5. Experimental and modeled NO profiles of the 60-Torr,  $\text{NH}_3/\text{N}_2\text{O}/\text{Ar}$  flame. The experimental profiles are obtained by MB-MS (Q) and LIF (B).

A comparison between the calculated O-atom profiles with the LIF measured profile (profiles not shown) reveals that both VS and VS-modified profiles are shifted  $\sim 2$  mm away from the burner surface compared to the experimental one, suggesting that the calculations predict a slower chemistry than what is observed experimentally. Also, the experimental profile peaks at a height near 5 mm above the burner, then decays and slowly increases in the postflame region. In contrast, the VS calculations show that the O-atom profile reaches a plateau in the postflame starting at a height near 8 mm above the burner surface, compared to the VS-modified calculations which predict a decay of 15%, similar to that observed experimentally. The VS-modified rate calculations show that the peak rate of production at  $\sim 7$  mm above the burner surface corresponds to the maximum temperature rise. The net integrated rate of O-atom production from 0 to 30 mm is  $3.26 \times 10^{-8} \text{ mol}/(\text{cm}^2\text{-s})$ . The reaction  $\text{N}_2\text{O} + \text{M} = \text{NO} + \text{O} + \text{M}$  accounts for 87% of the O-atom production flux, whereas  $\text{NO} + \text{N} = \text{N}_2 + \text{O}$  and  $\text{NNH} + \text{O} = \text{NO} + \text{NH}$  account for 7% and 5%, respectively, of the O-atom production flux. The O-atoms are consumed primarily by reactions  $\text{NH}_2 + \text{O} = \text{HNO} + \text{H}$ ,  $\text{OH} + \text{OH} = \text{H}_2\text{O} + \text{O}$ ,  $\text{NH}_3 + \text{O} = \text{NH}_2 + \text{OH}$ , and  $\text{H}_2 + \text{O} = \text{H} + \text{OH}$  reactions, with the first two reactions accounting for 62% of its consumption.

Figure 6 shows the calculated and measured  $O_2/Ar$  profiles. The shape of the  $O_2/Ar$  profile is predicted rather well by both the VS and VS-modified PREMIX calculations. Both calculations predict a flat region with a slight increasing slope in the postflame region, a trend similar to what is observed experimentally. The VS calculations, however, overpredict the value of the  $O_2/Ar$  ratio at 16.25 mm by about 61%. In contrast, the VS-modified calculations overpredict the  $O_2/Ar$  ratio by only 13%, just within our experimental uncertainty. VS-modified rate analysis of  $O_2$  reveals that  $\sim 60\%$  of this species is formed from the reaction  $H + O_2 = OH + O$  and  $\sim 39.6\%$  from the reaction  $N_2O + O = N_2 + O_2$ .  $O_2$  is consumed predominantly from the reactions  $NH + O_2 = HNO + O$ ,  $NO + O = N + O_2$ ,  $NH_2 + O_2 = HNO + OH$ ,  $O_2 + H + M = HO_2 + M$ , and  $NH + O_2 = NO + OH$ , with the first two reactions accounting for  $\sim 80\%$  of its consumption. The overall rate of  $O_2$  production is  $\sim 5.4$  times that of its consumption.

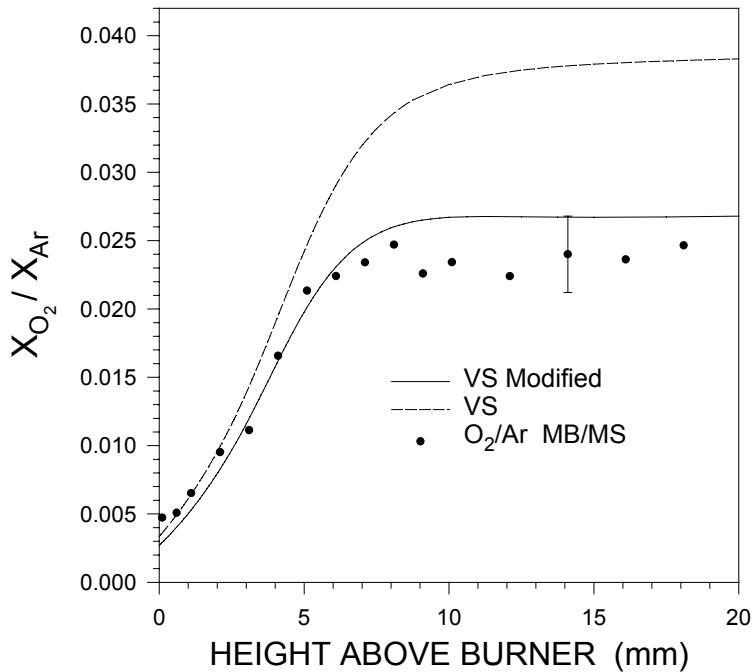


Figure 6. Experimental and modeled  $O_2$  profiles of the 60-Torr,  $NH_3/N_2O/Ar$  flame.

The PREMIX calculations are also performed using the GRI 3.0 chemical mechanism, with the supplied transport and thermodynamics databases as input [5]. The model calculations predict the observed  $NH_3$ ,  $N_2O$ ,  $H_2O$ , and  $N_2$  species mole fractions within 1% at 15 mm, similar to the PREMIX calculations using both the VS and VS-modified mechanisms. However, they overpredict the observed  $NO$  mole fraction by approximately a factor of 2 at 15 mm, and they underpredict the observed  $O_2$  mole fraction by  $\sim 17\%$  at its peak and by  $\sim 78\%$  at

15 mm. The model calculations also underpredict the O-atom mole fraction by ~50% at 15 mm, when both calculated and experimental profiles are normalized at ~6 mm. It should be noted, however, that the GRI mechanism is optimized for natural gas ignition.

---

## 4. Conclusion

---

A combined experimental and detailed modeling study of a  $\text{NH}_3/\text{N}_2\text{O}$  flame has been performed. The species concentration profiles of  $\text{NH}_3$ ,  $\text{N}_2\text{O}$ ,  $\text{N}_2$ ,  $\text{H}_2\text{O}$ ,  $\text{NH}$ ,  $\text{OH}$ ,  $\text{O}$ ,  $\text{NO}$ , and  $\text{O}_2$  have been measured by MB-MS, LIF, or both, and the flame temperatures have been measured by both thin-wire thermometry and OH and NH LIF. The experimental species mole fractions were compared with both NASA-Lewis equilibrium calculations and PREMIX calculations using the VS mechanism. Both calculations predicted the measured major species concentrations in the postflame within 1%. However, the equilibrium calculations did not adequately predict the postflame concentrations of NO and  $\text{O}_2$ , indicating that they were not chemically equilibrated. The PREMIX calculations adequately predicted the measured NO and OH profiles throughout the flame, but they overpredicted the  $\text{O}_2$  mole fraction ~60% in the postflame and did not adequately predict the shape of the O-atom profile. The experimental results were better predicted using a modified VS mechanism in which the rate expressions of the following reactions were altered to the limit of their experimental or calculated uncertainties: (1)  $\text{N}_2\text{O} + \text{H} = \text{OH} + \text{N}_2$ , (2)  $\text{NH}_2 + \text{O} = \text{HNO} + \text{H}$ , (3)  $\text{NH}_2 + \text{OH} = \text{NH} + \text{H}_2\text{O}$ , (4)  $\text{NH}_2 + \text{H} = \text{H}_2 + \text{NH}$ , (5)  $\text{NH}_3 + \text{OH} = \text{NH}_2 + \text{H}_2\text{O}$ , and (6)  $\text{NO} + \text{H} + \text{M} = \text{HNO} + \text{M}$ . Further experimental and modeling studies on the rate expressions of these reactions are thus recommended.

---

## 5. References

---

1. Venizelos, D. T., and R. C. Sausa. *Combustion and Flame*. Vol. 115, pp. 313–326, 1998, and references therein.
2. Sausa, R. C., G. Singh, G. W. Lemire, and W. R. Anderson (SSLA). *Twenty-Sixth Symposium (International) on Combustion*. The Combustion Institute, Pittsburgh, PA, pp. 1043, 1996, and references therein.
3. Vandooren, J., P. J. Van Tiggelen, and J.-F. Pauwels. *Combustion and Flame*. Vol. 109, pp. 647–668, 1997, and references therein.
4. Allen, M. T., R. A. Yetter, and F. L. Dryer. *Combustion and Flame*. Vol. 112, no. 3, pp. 302–311, 1998, and references therein.
5. Bowman, C. T., R. K. Hanson, D. F. Davidson, W. C. Gardiner, V. Lissianski, G. P. Smith, D. M. Golden, M. Frenklach, and M. Goldenberg. Gas Research Institute, Chicago, IL, <[http://euler.me.berkeley.edu/gri\\_mech/](http://euler.me.berkeley.edu/gri_mech/)>.
6. Svehla, R. A., and B. J. McBride. NASA-TN-D-7057, NASA Glenn (formerly Lewis), Cleveland, OH, January 1973.
7. Kee, R. J., J. F. Grcar, M. D. Smooke, and J. A. Miller. SAND-85-8240, Sandia National Laboratories, Livermore, CA, December 1985; reprinted March 1991.
8. Kee, R. J., F. M. Rupley, and J. A. Miller. SAND-89-8009, Sandia National Laboratories, Livermore, CA, September 1989.
9. Kee, R. J., F. M. Rupley, and J. A. Miller. SAND-87-8215, Sandia National Laboratories, Livermore, CA, April 1987.
10. Kee, R. J., G. Dixon-Lewis, J. Warnatz, M. E. Coltrin, and J. A. Miller. SAND-87-8246, Sandia National Laboratories, Livermore, CA, November 1988.
11. Miller, J. A., and C. T. Bowman. *Progress in Energy and Combustion Science*. Vol. 15, pp. 287–338, 1989.
12. Mertens, J. D., A. Y. Chang, R. K. Hanson, and C. T. Bowman. *International Journal of Chemical Kinetics*. Vol. 23, pp. 173–196, 1991.
13. Davidson, D. F., K. K. Kohse-Höinghaus, A. Y. Chang, and R. K. Hanson. *International Journal of Chemical Kinetics*. Vol. 22, pp. 513–535, 1990, and references therein.
14. Bozzelli, J. W., and A. M. Dean. *International Journal of Chemical Kinetics*. Vol. 27, pp. 1097–1109, 1995.

15. Anderson, W. R., S. W. Haga, J. F. Nuzman, and A. Kotlar. U.S. Army Research Laboratory SREAD and PREAD computer codes, U.S. Army Research Laboratory, Aberdeen Proving Ground, MD.
16. Brazier, C. R., R. S. Ram, and P. F. Bernath. *Journal of Molecular Spectroscopy*. Vol. 120, no. 2, pp. 381–402, 1986.
17. Dieke, G. H., and H. M. Crosswhite. *Journal of Quantitative Spectroscopy Radioactive Transfer*. Vol. 2, pp. 97–199, 1962.
18. Dimpfl, W. L., and J. L. Kinsey. *Journal of Quantitative Spectroscopy Radioactive Transfer*. Vol. 21, no. 3, pp. 233–241, 1979.
19. Marshall, P., T. Ko, and A. Fontijn. *Journal of Physical Chemistry*. Vol. 93, pp. 1922–1927, 1989.
20. Bozzelli, J. W., and A. M. Dean. “Combustion Chemistry of Nitrogen.” *Combustion Chemistry, 2nd ed.* Edited by W. C. Gardiner, New York: Springer Verlag, 1979.
21. Tsang, W., and J. T. Heron. *Journal of Physical Chemical Reference Data*. Vol. 20, pp. 609–663, 1991.
22. Votsmeier, M., S. Song, R. K. Hanson, and C. T. Bowman. *Journal of Physical Chemistry A*. Vol. 103, pp. 1566–1571, 1999.
23. Park, J., and M. C. Lin. *Journal of Physical Chemistry A*. Vol. 103, pp. 8906, 8907, 1999.

| <u>NO. OF COPIES</u> | <u>ORGANIZATION</u>   | <u>NO. OF COPIES</u> | <u>ORGANIZATION</u>   |
|----------------------|---|----------------------|---|
| 2                    | DEFENSE TECHNICAL<br>INFORMATION CENTER<br>DTIC OCA<br>8725 JOHN J KINGMAN RD<br>STE 0944<br>FT BELVOIR VA 22060-6218 | 3                    | DIRECTOR<br>US ARMY RESEARCH LAB<br>AMSRL CI LL<br>2800 POWDER MILL RD<br>ADELPHI MD 20783-1197   |
| 1                    | HQDA<br>DAMO FDT<br>400 ARMY PENTAGON<br>WASHINGTON DC 20310-0460   | 3                    | DIRECTOR<br>US ARMY RESEARCH LAB<br>AMSRL CI IS T<br>2800 POWDER MILL RD<br>ADELPHI MD 20783-1197 |
| 1                    | OSD<br>OUSD(A&T)/ODDR&E(R)<br>DR R J TREW<br>3800 DEFENSE PENTAGON<br>WASHINGTON DC 20301-3800                        |                      | <u>ABERDEEN PROVING GROUND</u>  |
| 1                    | COMMANDING GENERAL<br>US ARMY MATERIEL CMD<br>AMCRDA TF<br>5001 EISENHOWER AVE<br>ALEXANDRIA VA 22333-0001            | 2                    | DIR USARL<br>AMSRL CI LP (BLDG 305)   |
| 1                    | INST FOR ADVNCD TCHNLGY<br>THE UNIV OF TEXAS AT AUSTIN<br>3925 W BRAKER LN STE 400<br>AUSTIN TX 78759-5316            |                      |   |
| 1                    | US MILITARY ACADEMY<br>MATH SCI CTR EXCELLENCE<br>MADN MATH<br>THAYER HALL<br>WEST POINT NY 10996-1786                |                      |   |
| 1                    | DIRECTOR<br>US ARMY RESEARCH LAB<br>AMSRL D<br>DR D SMITH<br>2800 POWDER MILL RD<br>ADELPHI MD 20783-1197             |                      |   |
| 1                    | DIRECTOR<br>US ARMY RESEARCH LAB<br>AMSRL CI AI R<br>2800 POWDER MILL RD<br>ADELPHI MD 20783-1197                     |                      |   |

NO. OF  
COPIES   ORGANIZATION

ABERDEEN PROVING GROUND

30   DIR USARL  
      AMSRL WM BD  
      W R ANDERSON  
      R A BEYER  
      A L BRANT  
      S W BUNTE  
      C F CHABALOWSKI  
      L M CHANG  
      T P COFFEE  
      J COLBURN  
      P J CONROY  
      R A FIFER  
      B E FORCH  
      B E HOMAN  
      S L HOWARD  
      P J KASTE  
      A J KOTLAR  
      C LEVERITT  
      K L MCNESBY  
      M MCQUAID  
      M S MILLER  
      A W MIZIOLEK  
      J B MORRIS  
      J A NEWBERRY  
      M J NUSCA  
      R A PESCE-RODRIGUEZ  
      G P REEVES  
      B M RICE  
      R C SAUSA (3 CPS)  
      A W WILLIAMS

# REPORT DOCUMENTATION PAGE

Form Approved  
OMB No. 0704-0188

Public reporting burden for this collection of information is estimated to average 1 hour per response, including the time for reviewing instructions, searching existing data sources, gathering and maintaining the data needed, and completing and reviewing the collection of information. Send comments regarding this burden estimate or any other aspect of this collection of information, including suggestions for reducing this burden, to Washington Headquarters Services, Directorate for Information Operations and Reports, 1215 Jefferson Davis Highway, Suite 1204, Arlington, VA 22202-4302, and to the Office of Management and Budget, Paperwork Reduction Project(0704-0188), Washington, DC 20503.

|  |  |   |   |  |
|--|--|---|---|--|
| 1. AGENCY USE ONLY (Leave blank)   |  | 2. REPORT DATE<br>July 2002                             | 3. REPORT TYPE AND DATES COVERED<br>Final, January 1997-June 2002 |  |
| 4. TITLE AND SUBTITLE  |  |   | 5. FUNDING NUMBERS<br>622618.H80                                  |  |
| 6. AUTHOR(S)<br>Demetris T. Venizelos* and Rosario C. Sausa  |  |   |   |  |
| 7. PERFORMING ORGANIZATION NAME(S) AND ADDRESS(ES)<br>U.S. Army Research Laboratory<br>ATTN: AMSRL-WM-BD<br>Aberdeen Proving Ground, MD 21005-5066   |  |   | 8. PERFORMING ORGANIZATION REPORT NUMBER<br>ARL-TR-2782           |  |
| 9. SPONSORING/MONITORING AGENCY NAMES(S) AND ADDRESS(ES)   |  |   | 10. SPONSORING/MONITORING AGENCY REPORT NUMBER                    |  |
| 11. SUPPLEMENTARY NOTES<br>* Postdoctoral Research Associate, National Research Council, U.S. Army Research Laboratory, Aberdeen Proving Ground, MD 21005  |  |   |   |  |
| 12a. DISTRIBUTION/AVAILABILITY STATEMENT<br>Approved for public release; distribution is unlimited.  |  |   | 12b. DISTRIBUTION CODE  |  |
| 13. ABSTRACT (Maximum 200 words)<br>Experimental and chemical modeling studies of a 60-Torr, NH <sub>3</sub> /N <sub>2</sub> O/Ar flame are performed in order to provide further testing and refinements of a detailed chemical mechanism developed previously in our laboratory. This mechanism, which is denoted as VS, consists of 87 reactions and 20 species. Flame temperatures are measured with a coated thin-wire thermocouple and by rotational analyses of OH and NH laser-induced fluorescence (LIF) spectra. Species concentration profiles of NH <sub>3</sub> , N <sub>2</sub> O, N <sub>2</sub> , H <sub>2</sub> O, NO, O <sub>2</sub> , NH, O, and OH are recorded using molecular beam-mass spectrometry, LIF, or both. The experimental species concentrations are compared to those obtained with both equilibrium and PREMIX flame code calculations. The NH <sub>3</sub> /N <sub>2</sub> O mixture equilibrium calculations agree very well with both the PREMIX and measured postflame N <sub>2</sub> and H <sub>2</sub> O concentrations but underpredict the postflame NO concentration and overpredict the O <sub>2</sub> concentration. The PREMIX calculations predict very well the shapes of the experimental NH <sub>3</sub> , N <sub>2</sub> O, N <sub>2</sub> , H <sub>2</sub> O, NO, OH, and NH profiles throughout the flame but do not adequately predict the shape of the O-atom profile and overpredict the O <sub>2</sub> concentration by ~60% at 16.25 mm, suggesting that the VS mechanism requires some refinement. A VS-modified mechanism, which provides better agreement with the experimental results, is proposed. In this mechanism, the rate constants of the following reactions are altered to the limit of their experimental or calculated uncertainties: (1) N <sub>2</sub> O + H = OH + N <sub>2</sub> , (2) NH <sub>2</sub> + O = HNO + H, (3) NH <sub>2</sub> + OH = NH + H <sub>2</sub> O, (4) NH <sub>2</sub> + H = H <sub>2</sub> + NH, (5) NH <sub>3</sub> + OH = NH <sub>2</sub> + H <sub>2</sub> O, and (6) NO + H + M = HNO + M. |  |   |   |  |
| 14. SUBJECT TERMS  |  |   | 15. NUMBER OF PAGES<br>23   |  |
|  |  |   | 16. PRICE CODE  |  |
| 17. SECURITY CLASSIFICATION OF REPORT<br>UNCLASSIFIED  | 18. SECURITY CLASSIFICATION OF THIS PAGE<br>UNCLASSIFIED | 19. SECURITY CLASSIFICATION OF ABSTRACT<br>UNCLASSIFIED | 20. LIMITATION OF ABSTRACT<br>UNCLASSIFIED                        |  |

NSN 7540-01-280-5500

17

Standard Form 298 (Rev. 2-89)  
Prescribed by ANSI Std. Z39-18 298-102

INTENTIONALLY LEFT BLANK.